



Effect of Water Depth and Swell Parameters on Wave Propagation in the Coastal Zone of Benin

Bernard N. Tokpohozin ^{a,b,c*},
Djonoumawou M. G. F. Chidikofan ^c,
Fernando Y. J. Kpomahou ^d, Christian D. Akowanou ^{a,c},
Mathias A. Houékpohéha ^b, Guy H. Houngué ^e
and et Basile B. Kounouhéwa ^{b,e}

^a Higher National Institute of Preparatory Classes for Engineering Studies (INSPEI / UNSTIM) of Abomey, Republic of Benin.

^b Institute of Mathematics and Physical Sciences (IMSP/UAC) 01BP 613 Porto-Novo, Republic of Benin.

^c Laboratory of Sciences, Engineering and Mathematics (LSIMA/UNSTIM), Abomey, Republic of Benin.

^d Higher Normal School of Technical Education (ENSET / UNSTIM) of Lokossa BP 133 Lokossa, Republic of Benin.

^e Department of Physics (FAST) and Materials Sciences Doctoral Training, (FDSM / UAC), Republic of Benin.

Authors' contributions

This work was carried out in collaboration among all authors. Authors BNT and FYJK designed the study, performed the statistical analysis, and wrote the protocol and the first draft of the manuscript. The eBBK supervised and coordinated the work. Authors DMGFC, CDA, MAH, GHH performed the calculations and analyses of the study. All co-authors read and gave final approval for publication. All authors read and approved the final manuscript.

Article Information

DOI: <https://doi.org/10.9734/psij/2024/v28i5846>

Open Peer Review History:

This journal follows the Advanced Open Peer Review policy. Identity of the Reviewers, Editor(s) and additional Reviewers, peer review comments, different versions of the manuscript, comments of the editors, etc are available here: <https://www.sdiarticle5.com/review-history/120245>

*Corresponding author: E-mail: donaelfreed@gmail.com;

ABSTRACT

The coastal zone is studied as a morphodynamic system in the present work. A morphodynamic system comprises a geomorphological entity that adjusts its morphology in response to variations in a dynamic component. In recent years, particularly from 2015 to 2016, strong swells have been observed and have induced the destruction of coastal infrastructure and strong coastal erosion in the Gulf of Guinea, particularly Benin. Following this observation, our study is carried out to understand the origin of these strong events. Through this work, we tried to highlight the effect of water depth and swell parameters on wave propagation using experimental models from the literature. For this reason, MATLAB and Mathematica software were used for simulations. It can be said from the results obtained that the wave height has a considerable effect on the wave profile. The variation in water depth as a function of distance from the bed shows that it significantly affects the wave and its components.

Keywords: Wave simulation; water depth; swell; wave propagation; Benin coastal zone.

SCIENTIFIC NOTATION TABLES

v	: Ocean WATER FLOW VELOCITY (m/s)
ρ	: Density of Sea Water (kg/m ³)
Φ	: Velocity Potential in the Ocean (m ² /s)
η	: Vertical Elevation of the Water Level Relative to the Reference (m)
β	: Inclination of the Seabed Relative to the Horizontal (Rad)
γ	: Hydrodynamic Pressure (Pa)
g	: Acceleration of Gravity (m/s ²)
H	: Crest-to-trough Height of the Swell (m)
H_0	: Crest-to-trough Height of the Offshore Swell (m)
H_d	: Crest-to-trough Height of the Swell at the Breaking Point (m)
H_s	: Significant crest-to-trough Swell Height (m)
H_{max}	: Maximum Crest to trough Height of the Swell (m)
H_{min}	: Minimum Crest-to-trough Wave Height (m)
T_m	: Average Swell Period (s)
T_p	: Peak Wave Period (s)
$L = \frac{2\pi}{k}$: Wavelength of the Swell (m)
$T = \frac{2\pi}{\omega}$: Swell Period (s)
d	: Near Sea Surface-bottom Distance in Coastal Zones (m)
\vec{r}	: Position Vector of a Point Located on the Free Surface
V_g	: Group Swell Velocity (m/s)
V_ϕ	: Swell Phase Velocity (m/s)
V_x	: Horizontal Velocity of the Water Particles Struck by the Swell
V_z	: Vertical Velocity of the Water Particles Struck by the Swell

K_R	: Refraction Coefficients
K_S	: Shoaling Coefficients
A_x	: Horizontal Accelerations of Water Particles Struck by the Swell
A_z	: Vertical Acceleration of Water Particles Struck by the Swell
L_x	: Horizontal Movement of Water Particles Struck by the Swell
L_z	: Vertical Movement of Water Particles Hit by the Swell
MCA	: Millenium Challenge Account

1. INTRODUCTION

Comprehensive theoretical research on the propagation of waves in Benin's coastal areas could yield vital information for the region's coastal risk management and planning. [1]. The study of swell and wave propagation in the coastal zone of Benin involves understanding various factors that influence wave behavior, such as wind patterns, local water depth, coastal morphology, fetch, tide, ocean currents, and oceanographic conditions [2]. A theoretical study typically involves mathematical modeling and simulation to predict wave characteristics along the coast of Benin. Studying the ocean as a whole requires bridges linking the transversal skills of the different sciences in this case theoretical physics through modeling and analysis which lead to understanding and the search for solutions to the consequences of the increase in the level of the sea [1]. Mathematical theories, at the basis of all theoretical knowledge of the physical functioning of our environment,

which deal with waves, have developed and become more complex. They represent many phenomena linked to waves based on hypotheses developed from the general equations of fluid mechanics, and now make it possible to study ever more sophisticated problems analytically and numerically [3]. Overall, a theoretical study on swell and wave propagation in the coastal zone of Benin requires a multidisciplinary approach integrating oceanography, meteorology, hydrodynamics, and coastal engineering to provide valuable information for coastal management and decision-making [4]. The most spectacular physical manifestation occurring in the ocean is undoubtedly the swell. The coastline of Benin has suffered severe erosion for several years [5]. This phenomenon could be explained by a hydrodynamic dominated mainly by swells generated by the winds as well as a sandy coastline subject to a local microtidal type tide and a seasonal evolution of the intensity of the swells. In short, the coast of Cotonou in Benin is subject to two swell regimes: short swells (less energetic) generated by local winds and long swells (very energetic) generated in the South Atlantic which are the engine of one of the most significant coastal drifts in the world, from west to east [6]. In Cotonou, coastal transit is caused by the oblique attack of north-east or east-north-east swells during different storms [5]. Under the action of currents, winds, or swells, the solid particles, that form the sediments encountered in rivers and along coastlines, can be torn from the seabed, suspended, or transported over distances. More or less large and deposited in calm areas. These interactions are extremely complex in nature and the sedimentary movements that can be observed depend on multiple parameters. Velocity gradients in the fluid, vortices, bottom geometry, bank lines, nature of materials, thickness on the bedrock, porosity, and cohesion of the deposits, characteristics of the fluid... Will intervene in the conditions of erosion and transport of the materials. All these parameters, in addition, will not be constant over time but will undergo fluctuations. The swell in the fluid mass will cause the sediments to flow in certain situations in a mass direction toward privileged sectors due to reactions from translational and compensatory currents, return currents, orbital movements on the seabed, and coastal or return currents. On the sea surface, the friction of the local wind causes the water surface to move and generate ripples [1,7]. This 'sea of wind' is the superposition of several sinusoidal waves,

forming 'irregular' waves [2,4]. Under the effect of pressure gradients associated with gravity and induced by these variations in water height, these waves then propagate and are called gravity waves, or surface waves. These waves turn into swells when they propagate. The swell is thus the part of the sea state characterized by its absence of a relationship with the local wind. As part of this study, no distinction will be made between swell and waves, these two terms will define the sea state arriving on the shore. The land-sea interface is an extremely fragile environment. Coastlines, interfaces between land and sea, are places of great biological and landscape diversity, subject to strong pressures from natural elements and human beings. In the coastal zone, the most dynamic zones are the internal surf and swash zones [5]. The swash zone is of fundamental importance in the study of the coastal zone. The internal surf zone thus represents the border between the emerged part of the beach and the breaking zone. The internal surf zone and the swash zone thus form the very last zone of the beach where the waves will dissipate or reflect their remaining energy [1,8]. Throughout the world, coastlines are threatened by the combination of a multitude of factors, sometimes natural and most often anthropogenic. Thus, to the local disturbances caused to coastal areas by port infrastructures, dams, sediment collection from the beach, or even urban expansion, are added the global consequences of climate change, including the certain rise in the level of oceans and the probable amplification of devastating marine weather conditions. The direct consequence of global warming, the rise in ocean levels will have obvious consequences on coastal erosion in the decades to come. It is thus estimated, on a global scale, that sea levels could rise between 10 and 25 cm over the last century and 28 and 98 cm by 2100 according to estimates from the IPCC (Intergovernmental Panel on Climate Change). Climate change presented in their ar5 assessment report, based on different warming scenarios (IPCC, 2014) [1,8]. In Cotonou, since 2011, it was recently calculated that the average increase in sea level was 3.2 mm year⁻¹, which is close to the global values obtained over a similar period (IPCC, 2014) [9]. The simplest mathematical representation assuming the water waves used for the simulation is given as follows: two-dimensional (2-D), small amplitude, sinusoidal, and progressively definable by their amplitude and wave period in a depth of water given. In the simple representation of swells/waves, the movements and displacements

of swell/wave, the kinematics (i.e., velocities and accelerations of swell/wave), and the dynamics (i.e., wave/wave pressure and resultant forces and moments) are determined for technology design evaluations. When the wave amplitude becomes larger, simple treatment cannot be scaled. For regular swell/wave, we consider the 2-D approximation of the ocean surface deviated from a pure sinusoid [8]. This representation requires more complicated mathematical theories. These theories become non-linear and allow the formulation of swells/waves that are not sinusoidal in shape; for example, flat troughs and sharp ridges in shallow water when swells/waves are relatively high. The simplest swell/wave theory is first order and small amplitude, or the airy theory which is called

the linear theory [3]. This representation requires more complicated mathematical theories.

2. MATERIALS AND METHODS

2.1 Presentation of the Study Site

The coastal zone of Benin, between 6°15 and 6°38 north latitude, is part of the coastal sedimentary basin, the oldest of which dates back to the Cretaceous. Benin is a coastal state in the Gulf of Guinea (Fig. 1a). The coastline generally presents weak concavities oriented towards the ocean on this coast. There is increasing erosion towards the east. The climate is subequatorial with two dry seasons and two rainy seasons [4,8,10].

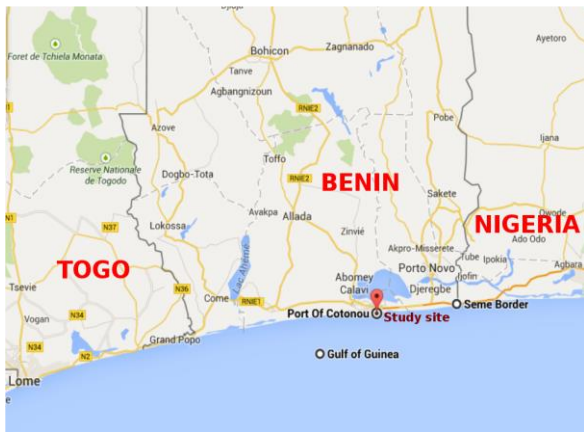


Fig. 1a. Geographical location of the coastal zone of Benin in the Gulf of Guinea

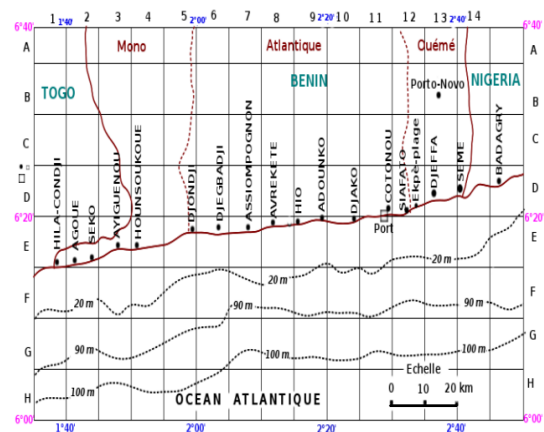


Fig. 1b. Bathymetric map of the Benin coastal zone



Fig. 1c. Image of Benin's coastal strip

In the coastal zone of Benin, there is no major obstacle that could significantly modify the direction of wave propagation ($\theta \approx \theta_o$) [8]. The average slope in the shoaling zone on this site is $p = \tan\beta \approx \frac{90}{2000} = 0,045$ [2] (Fig. 1b). In Benin, the swells which propagate towards the coast have a period T which varies between 10 s and 14 s and whose peak period is $T_p = 11.50\text{ s}$. Experimental measurements have shown that these waves break at the point of local depth d_b such that $4\text{ m} \leq d_b \leq 5\text{ m}$ and that their period oscillates between 9 s and 15 s [11]. Their heights vary almost sinusoidally and have two maxima and two minima on the same day. These heights vary between 0.6 m and 1.4 m . The maxima are observed around 5 a.m and 5 p.m GMT and the minima around 00 a.m and 12 p.m [12]. From data measurements relating to swell carried out at the autonomous port of Cotonou, at time intervals of five minutes over four consecutive years (June 2015 to April 2016) and obtained from the Institute of Fisheries and Oceanographic Research of Benin (IRHOB) of the Beninese Center for Scientific and Technical Research (CBRST), we have:

- Performs analysis of wave statistics on the coast of Benin.
- Simulated the temporal evolution of wave parameters such as the significant height $H_s\text{ (m)}$, the period of the peak $T_p\text{ (s)}$ and the direction of the peak $Dir\text{ (}^\circ\text{)}$.

- Shown the evolution of the vertical elevation η of the sea surface as a function of local water depth and compare swell profiles as a function of time in the different areas. For the study of swell propagation on this site, the abscissa axis is oriented in the East-West direction and the ordinate axis in the North-South direction as shown in Fig. 2:

The coastal strip of Benin is oriented in the South-West-West direction and thus tilts at an angle $\theta_o = 20^\circ$ approximately about the West-East direction [4].

2.2 Equations to Solve the Problem

- The movement of fluids (air and ocean) obeys the following Navier-Sokes equation [7].

$$\frac{\partial \vec{v}_i}{\partial t} + (\vec{v}_i \cdot \nabla) \vec{v}_i + \frac{1}{\rho_i} (\nabla P_i) - \vec{g} - \frac{\mu}{\rho_i} (\nabla^2 \vec{v}_i) = 0 \quad \text{with } i = 1, 2 \quad (1)$$

Irrotational and incompressible coastal flow can be modeled using Euler's equations in 3 dimensions. The strong non-linear nature of these equations prevents us from directly applying a numerical solution method. We must therefore simplify them before applying a numerical scheme. The viscosity in these two media being very negligible [13] and for surface waves, the convective term is negligible ($\mu \ll \rho_i$) compared to the acceleration $(\vec{v}_i \cdot \nabla) \vec{v}_i \ll \frac{\partial \vec{v}_i}{\partial t}$ [1].

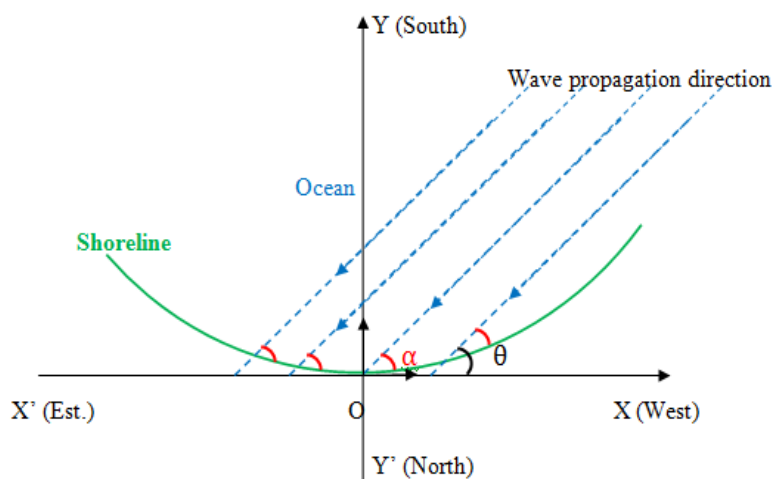


Fig. 2. Schematization of the study benchmark and direction of wave propagation in the Benin coastal zone

The oceanic environment is an incompressible fluid ($div(\vec{v}) = 0$), the flow is potential ($\vec{v} = \vec{\nabla}\phi$) and for a perfect fluid, we show that an irrotational disturbance remains so indefinitely. We can apply this theorem to the movement of waves whose flow will be assumed to be zero rotational (irrotational) $\overline{rot}(\vec{v}) = \vec{0}$ [1] where \vec{v} is the speed of a water particle driven by the flow and $\phi_2 = \phi$ the scalar potential of the velocities in the ocean and ϕ_1 that of the atmosphere. Thus, we obtain the Laplace equation below [14] $\Delta\phi = 0$. The solution of equation (1) allows us to find the dynamic pressure Y [15].

$$Y = -\rho \left(\frac{\partial\phi}{\partial t} \right) \quad (2)$$

- The area in which the effect of the Airy or Stokes swell (swell of very small amplitude compared to their wavelength) is felt is such [15,16].

$$\begin{cases} -\infty \leq x \leq +\infty \\ -\infty \leq y \leq +\infty \\ -d \leq z \leq 0 \end{cases} \quad (3)$$

- A water particle at a point on the free surface has a vertical speed $v_z = \frac{\partial\eta}{\partial t}$ along the vertical axis. The kinematic condition in $z = \eta$ gives [7].

$$\left(\frac{\partial\phi}{\partial z} \right)_{(z=\eta)} = \left(\frac{\partial\phi_i}{\partial z} \right)_{(z=\eta)} = \frac{\partial\eta}{\partial t} \quad (4)$$

- The swell being a surface wave, its effect disappears after a certain depth ($z = -d$). The condition of non-penetration to the bottom amounts to [2,8].

$$v_z(z = -d) = 0 \Rightarrow \left(\frac{\partial\phi}{\partial z} \right)_{(z=-d)} = 0 \quad (5)$$

- The dynamic condition at $z = \eta$ due to the existence of pressure and gravity forces at altitude z is written [15,16].

$$\left[g\eta + \frac{\partial\phi}{\partial t} \right]_{z=0} = 0 \Rightarrow \left[\frac{\partial^2\phi}{\partial t^2} + g \frac{\partial\phi}{\partial z} \right]_{z=0} = 0 \quad (6)$$

- The direction of wave propagation is almost rectilinear. It is assimilated to the axis (O, \vec{i}) and the average vertical elevation of the free surface is zero over a period.

$$\int_t^{t+T} \eta(\vec{r}, t) dt = \int_x^{x+L} \eta(\vec{r}, t) dx = 0 \quad (7)$$

- Any swell of wavelength propagates through three particular zones [16,17]. Offshore (deep water) when $d > \frac{L}{2}$; the lifting zone (Shoaling zone) if $\frac{L}{25} \leq d \leq \frac{L}{2}$; the breaking zone or shallow waters (Surf and Swash zones) for $0 \leq d \leq \frac{L}{25}$
- On the Beninese coast, the average slope in the Shaoling zone [2,12] is :

$$p = \tan(\beta) = \frac{90}{2000} = 0,045 \quad (8)$$

According to the bathymetric map along the Beninese maritime coast (Fig. 2) shows us that there is very little variation in the wavelength of the swells, either:

$$L = \frac{2\pi}{k} = \frac{gT^2}{2\pi} \quad (9)$$

2.3 Expression of $\phi(\vec{r}, t), \eta(\vec{r}, t)$ and the Group Velocity V_g

Solving equation (1) with conditions (3), (4), (5) and (6) gives complex results of which only the real parts below reflect the physical phenomenon [18,19].

$$\begin{cases} \phi_1 = \phi_1(x, y, z, t) = \frac{gH}{2w} e^{kz} \sin(\vec{k} \cdot \vec{r} - \omega t) \\ \phi_1 = \phi_1(x, y, z, t) = \frac{gH \cosh[k(z+d)]}{2w \cosh(kd)} \sin(\vec{k} \cdot \vec{r} - \omega t) \\ \eta = \eta(x, y, t) = \eta_0 \cos(\vec{k} \cdot \vec{r} - \omega t) = \frac{H}{2} \cos(\vec{k} \cdot \vec{r} - \omega t) \\ Y = -\rho \frac{\partial\phi}{\partial t} = \frac{\rho g H \cosh[k(z+d)]}{2 \cosh(kd)} \cos(\vec{k} \cdot \vec{r} - \omega t) \end{cases} \quad (10)$$

The fluid velocity in the x direction is: $V_x = \frac{\partial\phi}{\partial x}$ and the fluid velocity in the z direction is: $V_z = \frac{\partial\phi}{\partial z}$. The positions; velocities and accelerations of local fluids are:

$$\vec{V} \begin{cases} V_x = \frac{gHT}{2L} \frac{\cosh[2\pi(z+d)/L]}{\cosh(2\pi d/L)} \cos(\theta) \\ V_z = \frac{gHT}{2L} \frac{\sinh[2\pi(z+d)/L]}{\cosh(2\pi d/L)} \sin(\theta) \end{cases} \text{ with } \theta = \frac{2\pi x}{L} - \frac{2\pi t}{T} \quad (11)$$

The integration of this equation (11) gives the equations that parameterize the position of a water particle struck by the swell.

$$\vec{OM} \begin{cases} X = \frac{H}{2} \frac{\cosh[2\pi(z+d)/L]}{\cosh(2\pi d/L)} \sin(\theta) \\ Z = \frac{H}{2} \frac{\sinh[2\pi(z+d)/L]}{\cosh(2\pi d/L)} \cos(\theta) \end{cases} \text{ with } \theta = \frac{2\pi x}{L} - \frac{2\pi t}{T} \quad (12)$$

These equations express water particles' velocity and position components at any distance ($z + d$) above the bottom. They are periodic in x and t .

For a given value of the phase angle $\theta = 2\pi\left(\frac{x}{L} - \frac{t}{T}\right)$. The trajectory of the particles is therefore circular in infinite depth (offshore) and elliptical in shape that becomes more and more crushed as the bottom rises. The equations of system (11) generally parameterize the ellipses with major horizontal axis DD' and minor vertical axis d' verifying the equation:

$$\left(\frac{x}{DD'}\right)^2 + \left(\frac{z}{d'}\right)^2 = 1 \text{ with } \begin{cases} DD' = \frac{H}{2} \frac{\cosh[2\pi(z+d)/L]}{\cosh(2\pi d/L)} \\ d' = \frac{H}{2} \frac{\sinh[2\pi(z+d)/L]}{\cosh(2\pi d/L)} \end{cases} \quad (13)$$

This model established in 1804 by Gerstner is a rigorous solution for a fluid at infinite depth (Fig. 3a). Each fluid particle is supposed to rotate around a point with coordinates X_0, Z_0 , describing a circumference of radius R, decreasing exponentially with depth d .

The derivation of this equation (11) gives the equations that parameterize the accelerations of the particles of the fluid struck by the swell. The accelerations of the fluid particles are:

$$\begin{cases} A_x = \frac{gH}{L} \frac{\cosh[2\pi(z+d)/L]}{\cosh(2\pi d/L)} \sin(\theta) \\ A_z = -\frac{gH}{L} \frac{\sinh[2\pi(z+d)/L]}{\cosh(2\pi d/L)} \cos(\theta) \end{cases} \text{ with } \theta = \frac{2\pi x}{L} - \frac{2\pi t}{T} \quad (14)$$

And the movement of water particles is given by:

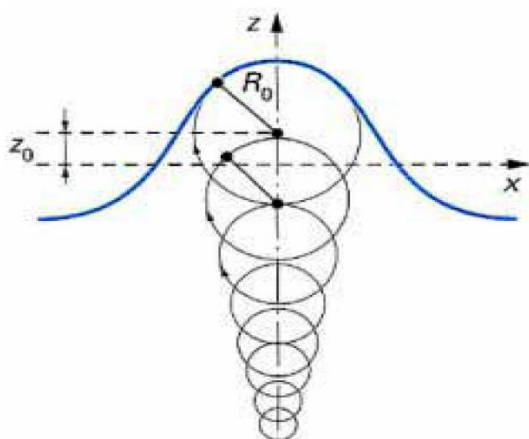


Fig. 3a. Trajectory of water particles in the Gerstner swell [20,21]

$$\begin{cases} \mathcal{L}_x = -\frac{HgT^2}{4\pi L} \frac{\cosh[2\pi(z+d)/L]}{\cosh(2\pi d/L)} \sin(\theta) \\ \mathcal{L}_z = \frac{HgT^2}{4\pi L} \frac{\sinh[2\pi(z+d)/L]}{\cosh(2\pi d/L)} \cos(\theta) \end{cases} \text{ with } \theta = \frac{2\pi x}{L} - \frac{2\pi t}{T} \quad (15)$$

The secondary external pressure under a wave is the sum of two pressure components, dynamic and static, and is given by:

$$Y' = \frac{\rho g H}{2} \frac{\cosh[2\pi(z+d)/L]}{\cosh(2\pi d/L)} \cos(\theta) - \rho g z + p_0 \text{ with } \theta = \frac{2\pi x}{L} - \frac{2\pi t}{T} \quad (16)$$

The equation for the water surface is given by:

$$\eta = \eta_1 + \eta_2 = \frac{H}{2} \cos\left(\frac{2\pi x}{L_1} - \frac{2\pi t}{T_1}\right) + \frac{H}{2} \cos\left(\frac{2\pi x}{L_2} - \frac{2\pi t}{T_2}\right) \quad (17)$$

And

$$\eta_{enveloppe} = \pm H \cos\left[\pi\left(\frac{L_2-L_1}{L_1 L_2}\right)x - \pi\left(\frac{T_2-T_1}{T_1 T_2}\right)t\right] \quad (18)$$

The swell dispersion relation according to the linear theory [22,23] is :

$$\omega^2 = gk \cdot \tanh(kd) \quad (19)$$

The phase (celerity) and group velocities of a swell are respectively [17,24].

$$\begin{cases} V_\varphi = \frac{\omega}{k} = \sqrt{\frac{g}{k} \tanh(kd)} \\ V_g = \frac{\partial \omega}{\partial k} = \frac{1}{2} \frac{\omega}{k} \left(1 + \frac{2kd}{\sinh(2kd)}\right) \end{cases} \quad (20)$$

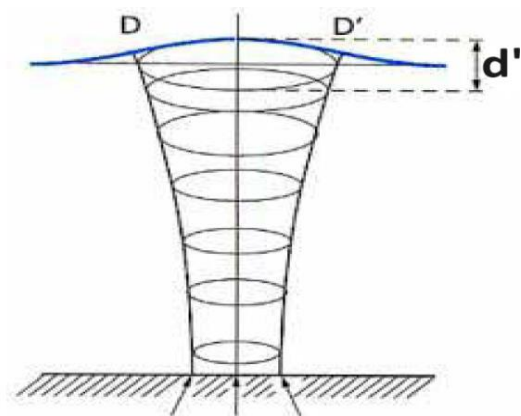


Fig. 3b. Trajectory of water particles in the Stokes swell [21]

Table 1. Waves classification

Classification	$\mu = d/L_0$	kd	$\tanh(kd)$
Deep Waters	1/2 to $+\infty$	π to $+\infty$	= 1
Shoaling zone	1/25 to 1/2	$\pi/10$ to π	$\tanh(kd)$
Shallow waters	0 to 1/25	0 to $\pi/10$	= kd

Note that an argument of the hyperbolic tangent $kd = 2\pi d/L_0$ is large, the $\tanh(kd)$ approaches 1, and for small values of kd , $\tanh(kd) \simeq kd$. Water waves are classified in Table 1 based on the relative depth criterion d/L_0 .

- In deep waters, $V_{g0} = \frac{1}{2}V_\varphi = \frac{gT}{4\pi}$ and $L_0 = \frac{gT^2}{2\pi}$ [25];
- In the Shoaling zone, $V_g = \frac{1}{2}\left(1 + \frac{2kd}{\sinh(2kd)}\right)\sqrt{\frac{g}{k}\tanh(kd)}$;
- In the shallow waters, $V_g = V_\varphi = \sqrt{gd}$ [26];

In the end, we have:

$$V_g(d) = \begin{cases} \frac{gT}{4\pi} & \text{if } \frac{d}{L_0} > \frac{1}{2} \\ \frac{1}{2}\left(1 + \frac{2kd}{\sinh(2kd)}\right)\sqrt{\frac{g}{k}\tanh(kd)} & \text{if } \frac{1}{25} \leq \frac{d}{L_0} \leq \frac{1}{2} \\ \sqrt{gd} & \text{if } 0 \leq \frac{d}{L_0} \leq \frac{1}{25} \end{cases} \quad (21)$$

Gold by posing $k = 2\pi/L_0$

$$V_g(d) = \begin{cases} \frac{gT}{4\pi} & \text{if } \frac{d}{L_0} > \frac{1}{2} \\ \frac{1}{2}\left(1 + \frac{4\pi d/L_0}{\sinh(4\pi d/L_0)}\right)\sqrt{\frac{gL_0}{2\pi}\tanh(2\pi d/L_0)} & \text{if } \frac{1}{25} \leq \frac{d}{L_0} \leq \frac{1}{2} \\ \sqrt{gd} & \text{if } 0 \leq \frac{d}{L_0} \leq \frac{1}{25} \end{cases} \quad (22)$$

2.4 Swell Height

In deep water, the swell height is constant and is $H = H_0 = cste$. In the Shoaling zone [7,8], $H = K_S K_R H_0$ Where

$$K_S = \sqrt{\frac{V_{g0}}{V_g}} = \left(\frac{2\pi d/L_0}{\cosh^2(2\pi d/L_0)} + \tanh(2\pi d/L_0)\right)^{\frac{1}{2}} \text{ and } K_R = \sqrt{\frac{\cos\theta_0}{\cos\theta}} \quad (23)$$

Are respectively the Shoaling and refraction coefficients, θ_0 and θ the directions of propagation of the wave before and after refraction. So we get, [12]:

$$H = H_0 \sqrt{\frac{\cos\theta_0}{\cos\theta}} \left(\frac{2\pi d/L_0}{\cosh^2(2\pi d/L_0)} + \tanh(2\pi d/L_0)\right)^{\frac{1}{2}} \quad (24)$$

The height of the swell decreases in the breaking zone [5,21] and According to P. Bonneton (2002), this height is given by:

In the end, we have:

$$H(d) = \begin{cases} H_o & \text{if } \frac{d}{L_0} > \frac{1}{2} \\ H_o \sqrt{\frac{\cos\theta_0}{\cos\theta} \left(\frac{2\pi d/L_0}{\cosh^2(2\pi d/L_0)} + \tanh(2\pi d/L_0) \right)^{-1/2}} & \text{if } \frac{d_b}{L_0} \leq \frac{d}{L_0} \leq \frac{1}{2} \\ H_o \left[\frac{2H_o}{T \tan\beta \sqrt{gd_b}} \left(\frac{d}{d_b} \right)^{-1/2} + \left(1 - \frac{2H_o}{T \tan\beta \sqrt{gd_b}} \right) \left(\frac{d}{d_b} \right)^{1/4} \right]^{-1} & \text{if } 0 \leq d \leq d_b \end{cases} \quad (25)$$

3. RESULTS AND DISCUSSION

3.1 Results

➤ The curves in Fig. 4 reveal the temporal distribution of the hydrodynamic parameters of the port of Cotonou from 2015 to 2016. The data observed every hour of the

parameters characterizing the state of the waves (significant height, peak direction, and peak period) at both anchorages from December 2015 to August 2016 are presented in Fig. 4.
 ➤ The following Fig. 5 shows us the comparison of wave profiles and physical quantities as a function of time.

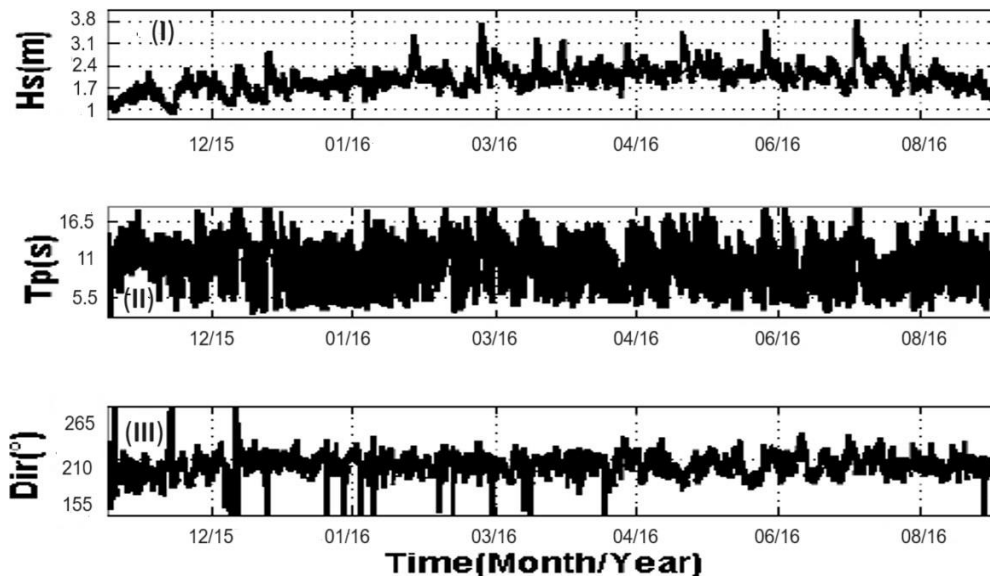


Fig. 4. Temporal evolution of the hydrodynamic parameters of the port of Cotonou: significant wave height (Hs) (I), peak period (Tp) (II), and direction (Dir) (III) between 2015 and 2016

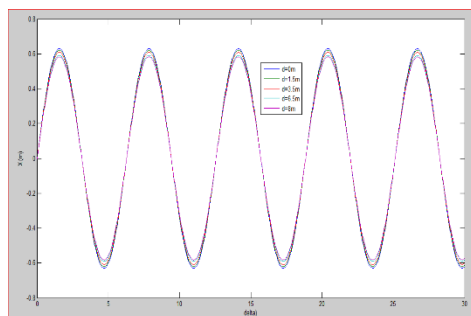


Fig. 5a. Variation of horizontal position X

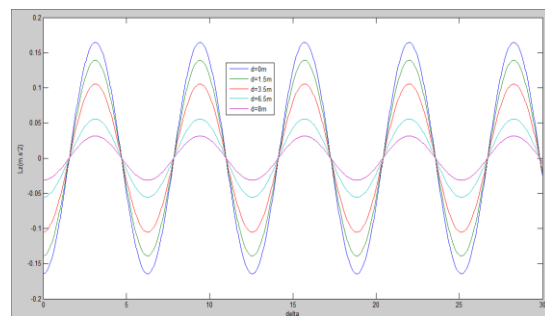


Fig. 5b. Variation of vertical position Z

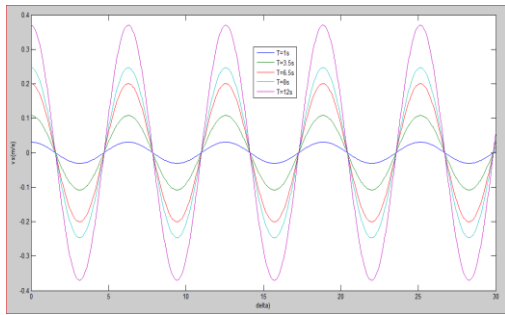


Fig. 5c. Variation of the horizontal velocity of water particles

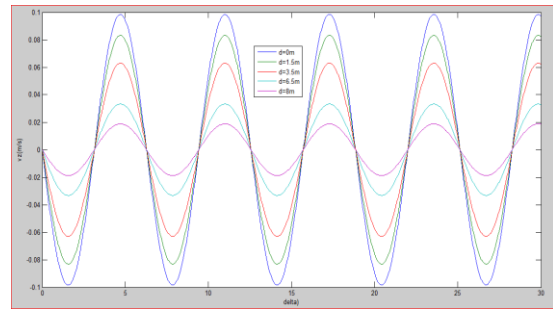


Fig. 5d. Variation of the vertical velocity of water particles

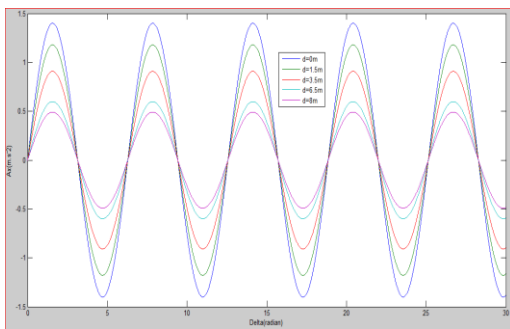


Fig. 5e. Variation of horizontal acceleration of water particles

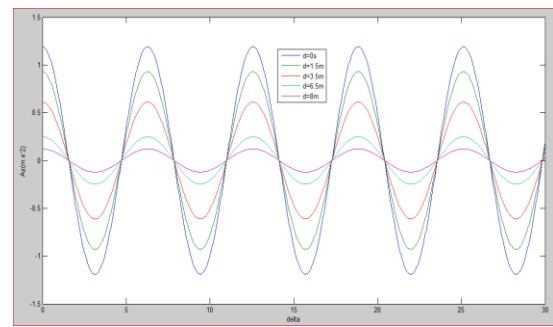


Fig. 5f. Variation of vertical acceleration of water particles

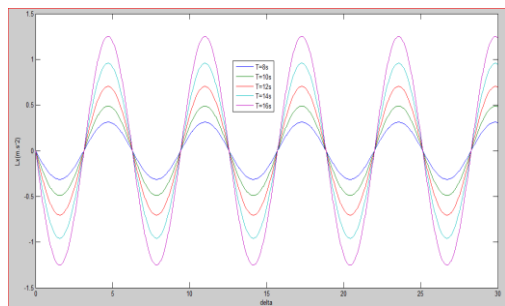


Fig. 5g. Variation in horizontal displacement of water particles to $d=cst$

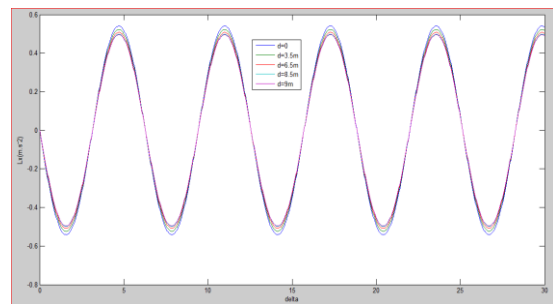


Fig. 5h. Variation in horizontal displacement of water particles to $T=cst$

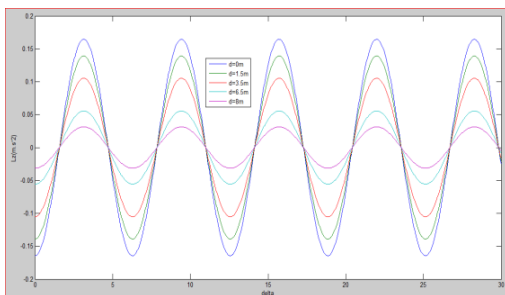


Fig. 5i. Variation of vertical displacement of water particles

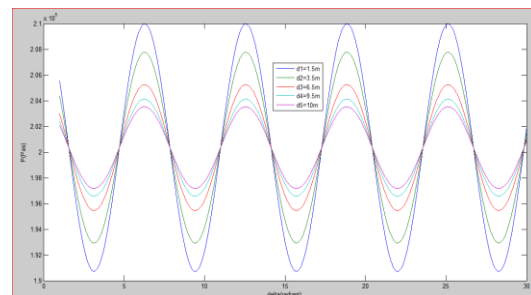


Fig. 5j. Variation of dynamic pressure

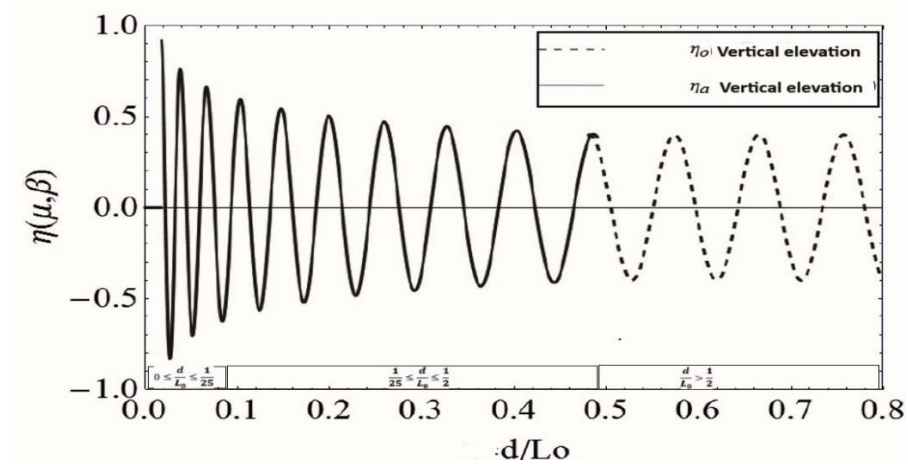


Fig. 6. Vertical elevation of the sea surface in deep water $\eta_0(d/L_0)$ and in the shoaling zone $\eta_a(d/L_0, \beta)$ in dimension two of the local water depth d/L_0

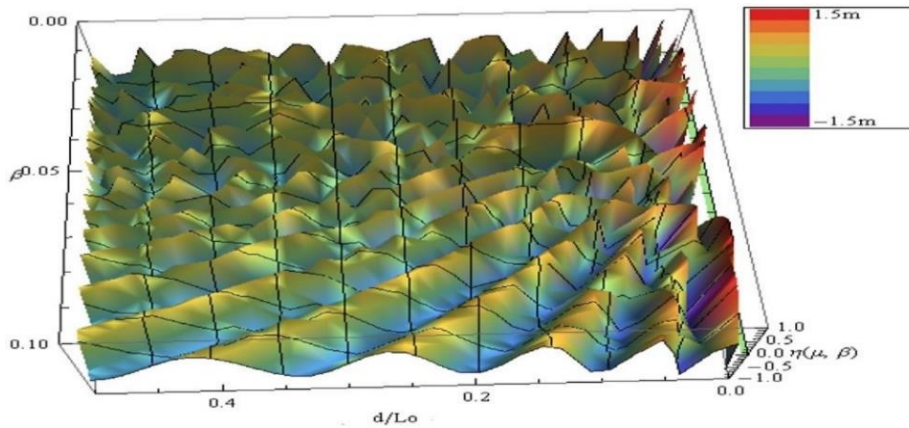


Fig. 6a. Vertical elevation $\eta_a(d/L_0, \beta)$ of the sea surface in the shoaling zone in 3D as a function of the local water depth d/L_0 and the seabed slope β

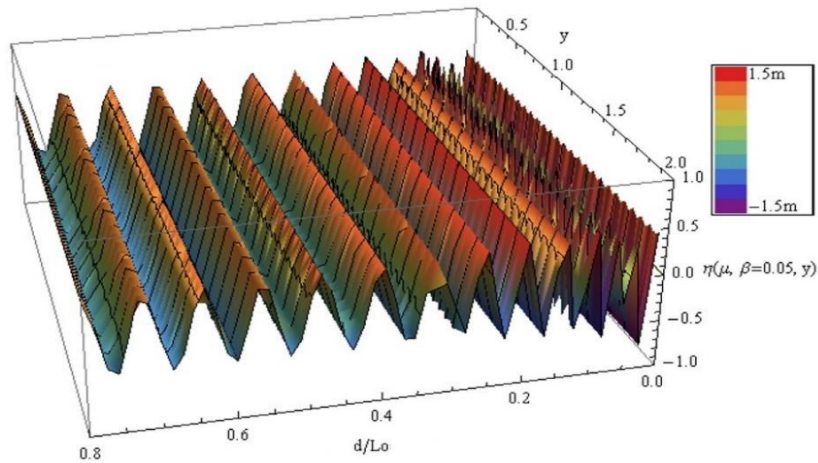


Fig. 6b. Vertical elevation of the marine surface offshore $\eta_0(d/L_0)$ and in the shoaling zone $\eta_a(d/L_0, \beta = 0, 05)$ in 3D of the local water depth d/L_0

- Figs. 6, 6a, and 6b, show the evolution of the vertical elevation of the sea surface as a function of the local water depth μ and the slope of the seabed β . The curve in Fig. 6 is a representation in dimension 2 (2D) whereas those of Figs. 6a and 6b are its representations in dimension 3 (3D).

3.2 Discussion

- It is important to note that the amplitude of the speed decreases exponentially with a coefficient proportional to the wave number k . Therefore, the orbital speed of waves with a larger period (smaller number of waves) will be more present at the bottom than that of waves with short periods (Figs. 3a and 3b). The waves induce an orbital movement in the water and the amplitude of this movement decreases with depth (Figs. 3a and 3b). In shallow water, the elliptical paths followed by water particles flatten to horizontal lines, particularly at the bottom, where there is no vertical flow. The trajectory of the particles is therefore circular in infinite depth (offshore) and elliptical becomes more and more crushed as the bottom rises.
- Fig. 4.I indicate a strong temporal variability of H_s extending from typical wind force values (minimum 0.71 m) to fairly energetic swells (maximum 3.22 m) during the years 2015 and 2016, some sequences exceptionally energetic with significant height values between 3.05 and 3.22m. This mixture of ocean regime and sea wind is corroborated by the maximum swell periods observed, varying between 5.50 and 15.66 s (Fig. 4.II). The observed wave peak periods vary between 4.38 and 17.85s with an average of 11.7s. The maximum direction of all waves varies very little (standard deviation of 2.38°) with an average direction of 211.5° clockwise from the north (dominant waves from the SSW sector) except on rare occasions (266 and 235° respectively in 2015 and 2016, (Fig. 4.III, we see a different grid (3,15° > 1,7°). The average height of all waves over the period (2015-2016). is 1.29 m and 9.30 m for the peak period. The analysis of the different curves (Fig. 4) of the wave parameters makes it possible to identify two phases: the first going from June to July characterized by waves of fairly strong energy ($H_{smoy} > 1,32m$ and $T_{p moy} > 11s$). The second phase goes from July to August, it is characterized by slightly less

energetic waves ($H_{smoy} < 1,1m$ and $3,4s < T_p < 16s$). The wave periods during the first phase are as high as the significant heights. In contrast, in the second phase, the wave height decreased with the increase in wind speed [2]. The waves are therefore characterized by energy spectra, which reveal characteristic quantities, with for example a significant height H_s , a significant period T_s , etc.... These spectra are broad for wind waves, and narrower for an already formed swell which continues to propagate far from its zone of generation by the wind.

- In Figs. 5a, 5b, it is noted that the calculated results for the depth water wave profile for linear waves are quite similar to nonlinear waves, thus the comparisons indicate that the currently obtained solutions deviate from the existing results of Cruz et al for regular linear waves, so some anomaly is expected between the present results and Cruz's solutions formulated for nonlinear waves. Water particle velocities under linear waves are greatest at the surface and decrease in magnitude with depth (Figs. 5c and 5d). The speed of wave propagation depends on their wavelength, their amplitude, and as they approach the coastline, the water depth (Figs. 5c and 5d). The phenomenon of wave propagation is therefore dispersive. Furthermore, the waves do not all propagate in the same direction, resulting in a sometimes chaotic appearance of the sea surface state. The directions of particle speeds are linked to the movement of the water surface. At the crest of the wave, the movement of the water is horizontal and in the direction of the wave. At the trough, the speed is reversed (by the same magnitude as at the peak in linear theory). Vertical velocities reach their maximum when water crossings occur. We notice that the velocities of the water particles increase (Figs. 5c and 5d) and the accelerations of the water particles decrease (Figs. 5e and 5f) from deep water to shallow water, this gives us a good agreement between these results and previous results for deep-water and shallow-water wave measurements. It can be said from the results obtained that the wave height has a considerable effect on the wave profile. Then, the crest has moved, the pressure is maximum at its summit and decreases going down in the direction of propagation (Fig. 5j). The pressure decreases, so the speed increases. On the

other hand, in the left part of the direction of propagation, the pressure increases from left to right (up to the trough), the pressure force acting under the wave crest is greater than the pressure force under the wave trough leading to a net effort over a wave period (Fig. 5j). Figs. 5a, 5b, 5c, 5d, 5e, 5f, 5g, 5h, show a good agreement between the speeds and accelerations of the current model, there is only a difference in the values.

- The analysis of the results, after several years of monitoring the morphodynamics of the Beninese beach, made it possible to highlight the link between the sea surface and the seabed. However, these results should be moderated due to the particularly favorable weather conditions (absence of erosive storms) observed since 2011. In the breaking zone where $d = 3m$, this potential also varies with a non-negligible average. The shoaling zone is therefore a zone of strong amplification of the energy power of the swell, while those of Surf and Swash are the zones of energy dissipation. These results show that the swells in Benin are more energetic in the shoaling zone. The curves of Figs. 6, 6a, and 6b, translate the variations of the vertical elevation of the free surface of the ocean according to the local water depth. Note that the curve of Fig. 6 represents dimension 2 (2D) while those of Figs. 6a and 6b are its representations in dimension 3 (3D). They confirm:

- The constancy of the various offshore parameters.
-
- Height amplification crest to the trough of the swells in the shoaling zone under the disturbing effect of the seabed.

The slope of this seabed causes the decrease or contraction of the wavelength. The curve of Fig. 6b, which represents the variations of the vertical elevation of the free surface of the ocean according to the local water depth $d = \mu L_o$ and the slope of the seabed β in the shoaling zone, reveals that the randomness accompanied by small oscillations on the surface of the swell is due to the variability of the slope of the seabed.

4. CONCLUSION

In the Gulf of Guinea at Cotonou, the swells are regular and have a constant average height $H_o =$

0,8m and an average period $T = 11s$ in deep waters. In the coastal zone, the disturbing effect of the seabed causes them to rise to the breaking point and it is the modified Boussinesq theory, proposed by Peregrine in 1967, makes it possible to model them. These swells become very energetic in this zone, their height is amplified and remains proportional to $(d^{-1/4})$. At the breaking point, the maximum height these swells reach varies between 1,7m and 2,5m. Their bathymetric surge, occurs at a position where the local water depth d_b oscillates between 1.6m and 4.5m very close to the coastline depending on the value of the slope of the seabed. This Breaking is a sudden energy discharge that induces and accentuates the phenomenon of coastal erosion. The waves are therefore characterized by energy spectra, which reveal characteristic quantities, with for example a significant height H_s , a significant period T_s , etc.... These spectra are broad for wind waves, and arrower for an already-formed swell which continues to propagate far from its zone of generation by the wind. Swells induce an orbital motion in the water and the amplitude of this motion decreases with depth. It is important to note that the amplitude of the velocity decreases exponentially with a coefficient proportional to the number of waves k . So, the orbital velocity of swells with a longer period (smaller wave number) will be more present at sea floor than that of waves with shorter periods. The propagation velocity of the swells depends on their wavelength, their amplitude and when approaching the coast, the water depth. The swells are therefore characterized by energy spectra, which show characteristic quantities, with for example a significant height H_s , a significant period T_s , etc Water particles also describe vertical circles which become progressively smaller with increasing depth, the decrease being exponential. The reason for describing simple waves is that they represent the basic solutions of the physical equations that govern waves on the sea surface and they are the building blocks for real wave fields occurring at sea. Actually, the idea of basic sinusoidal waves is widely applied to help in the comprehension and characterization of waves. Despite this simplified description, definitions and formulas derived from waves are intensively employed in practice and have proven their value. It can be said from the results obtained that the wave height has a considerable effect on the wave profile. It has a major impact on the wave and its constituent parts, as seen by the fluctuation in

water depth as a function of distance from the bed. From the present work we can say that the combination of the effects of height and depth together contribute to the understanding of the behavior of the wave and its velocities and accelerations of the water particles. Therefore, the orbital speed of waves with a larger period (smaller number of waves) will be more present at the bottom than that of waves with short periods. The speed of wave propagation depends on their wavelength, their amplitude, and as they approach the coast, the water depth. The phenomenon of wave propagation is therefore dispersive. Furthermore, the waves do not all propagate in the same direction, resulting in a sometimes chaotic appearance of the sea surface. The variation in the depth of the water as a function of the distance from the bed shows that it has a very significant effect on the wave and its components. Wave propagation is a phenomenon that is very sensitive to a large number of parameters, in particular, the speed of the waves after breaking v_g , their period T , their wavelength in deep waters L_0 , the slope of the seabed β , the crest to trough height of the swell H , the obliquity of the swell α , the local water depth d .

DISCLAIMER (ARTIFICIAL INTELLIGENCE)

Author(s) hereby declare that NO generative AI technologies such as Large Language Models (ChatGPT, COPILOT, etc) and text-to-image generators have been used during writing or editing of manuscripts.

DATA AVAILABILITY

The datasets generated during and/or analyzed during the current study are available from the authors at reasonable request.

ACKNOWLEDGEMENTS

The authors thank the Beninese Center for Scientific Research and Innovation (IRHOB/CBRSI) not only for supporting this research work but also for the data made available to us.

COMPETING INTERESTS

Authors have declared that no competing interests exist.

REFERENCES

1. Tokpohozin NB. Influence of swell on sedimentary dynamics in the coastal zone of Benin", Single doctoral thesis, University of Abomey-Calavi (UAC), Institute of Mathematics and Physical Sciences (IMSP); 2016.
2. Tokpohozin BN et al. Prospects for the characterization of the fundamental parameters linked to the energy spectrum of the aeolian sea state in Benin coastal zone. *Curr. J. Appl. Sci. Technol.* 2023, nov;42(42):19-35. DOI: 10.9734/cjast/2023/v42i424270.
3. Al-Dwairi ZN, Tahboub KY, Baba NZ, Goodacre CJ, et M Özcan. A comparison of the surface properties of CAD/CAM and conventional polymethylmethacrylate (PMMA). *J. Prosthodont.* 2019, avr;28(4): 452-457. DOI: 10.1111/jopr.13033.
4. Hervé Houngouè G, Kounouhewa BB, Almar R, Sohou Z, Lefebvre JP, et M Houépkonhéha. Waves forcing climate on bénin coast, and the link with climatic index, Gulf of Guinea (West Africa). *J. Coast. Res.* 2018, sept;81(sp1):130. DOI: 10.2112/SI81-017.1.
5. Tokpohozin NB, Kounouhewa B, Avossevou GYH, Houekpoheham A, et Awanou CN. Modelling of sediment movement in the surf and swash zones. *Acta Oceanol. Sin.* 2015, févr;34(2): 137-142. DOI: 10.1007/s13131-015-0610-2.
6. Almar R et al. The grand popo beach 2013 experiment, Benin, West Africa: from short timescale processes to their integrated impact over long-term coastal evolution. *J. Coast. Res.* 2014, avr;70:651-656. DOI: 10.2112/SI70-110.1.
7. Acclassato OG, Tokpohozin NB, Akowanou CD, Houékpohéha AM, Houngue GH, et Kounouhéwa BB. Study of dissipating of wave energy in the breakers zone of the gulf of guinea: Case of autonomous port of cotonou in Benin coastal zone. *J. Mod. Phys.* 2022;13(09):1272-1286. DOI: 10.4236/jmp.2022.139076
8. Noukpo Bernard T, Jean-Louis FC, Guy HH, Mathias HA, et KB Basile. Energetic power estimation of swells and orbital

- marine currents in benin coastal zone (Gulf of Guinea). *Int. J. Adv. Res.* 2023, févr;11(02)366-382.
DOI: 10.21474/IJAR01/16261.
9. Melet A, Almar R, Hemer M, G Le Cozannet, B Meyssignac, et P Ruggiero. Contribution of wave setup to projected coastal sea level changes. *J. Geophys. Res. Oceans.* 2020, août;125(8):e2020JC016078.
DOI: 10.1029/2020JC016078.
 10. Hounguè GH, Houépkonhéha MA, Tokpohozin NB, et BB Kounouhéwa. Wave energy potential assessment during recent extreme events observed on Benin's coastal area, Gulf of Guinea (West Africa). *Journal de physique de la SOAPHYS, Afrique de l'Ouest.* 2019;C19A15.
 11. Hounguè GH, Kounouhéwa BB, Houépkonhéha MA, Tokpohozin BN, et VI Madogni. Wave energy resources assessment offshore Benin from ERA Re-analysis: Gulf of Guinea. *Phys. Sci. Int. J.* 2018, nov;19(4):1-11.
DOI: 10.9734/PSIJ/2018/44226.
 12. Tokpohozin NB, Fannou JL, Houekpoheha AM, Hounguè HG, et BB Kounouhéwa. Statistical study of wave parameters : Sea states in the deep waters (offshore) of the gulf of guinea in benin. *Int. J. Curr. Res.* 2013, févr;15(02):23709-23719.
DOI: 10.24941/ijcr.44701.02.2023.
 13. Rabaud et MF Moisy. The Kelvin–Helmholtz instability, a useful model for wind-wave generation? *Comptes Rendus Mécanique.* 2020, nov;348(6-7):489-500.
DOI: 10.5802/crmeca.31.
 14. Aurélien Babarit, Jean-Marc Rousset, Hakim Mouslim, Judicaël Aubry, Hamid Ben Ahmed, et Bernard Multon. Chapter 4 wave prediction models », in Elsevier Oceanography Series., Elsevier. 1989;49: 75-105.
DOI: 10.1016/S0422-9894(08)70124-7.
 15. Clauss M, Nunn C, Fritz J, et J Hummel. Evidence for a tradeoff between retention time and chewing efficiency in large mammalian herbivores. *Comp. Biochem. Physiol. A. Mol. Integr. Physiol.* 2009, nov;154(3):376-38.
DOI: 10.1016/j.cbpa.2009.07.016.
 16. Chalikov D et D. Sheinin. Modeling extreme waves based on equations of potential flow with a free surface. *J. Comput. Phys.* 2005, nov ;(1)247-273.
DOI: 10.1016/j.jcp.2005.04.008.
 17. Isebe D et al. Une nouvelle approche pour la protection des plages : Application à la plage du Lido de Sète », in Xèmes Journées, Sophia Antipolis, Editions Paralia. 2008 ;263-272.
DOI: 10.5150/jngcgc.2008.025-I.
 18. Chen G, Chapron B, Ezraty R, et Vandemark D. A global view of swell and wind sea climate in the ocean by satellite altimeter and scatterometer. *Journal of atmospheric and Oceanic Technology.* 2002;1849-1859.
 19. Xu Y et X. Yu. Enhanced formulation of wind energy input into waves in developing sea. *Prog. Oceanogr.* 2020, juill;186:102376.
DOI: 10.1016/j.pocean.2020.102376.
 20. Alves JHGM. Numerical modeling of ocean swell contributions to the global wind-wave climate. *Ocean Model.* 2006;11(1-2): 98-122.
DOI: 10.1016/j.ocemod.2004.11.007.
 21. Jose-Henrique GMA. Numerical modeling of ocean swell contributions to the global wind-wave climate. *Ocean Modelling.* 2006;98-122.
 22. Castelle B, Bonneton P, Dupuis H, et N Sénéchal. Double bar beach dynamics on the high-energy meso-macrotidal french aquitanian coast: A review. *Mar. Geol.* 2007, nov;245(1-4): 141-159.
DOI: 10.1016/j.margeo.2007.06.001.
 23. Castelao RM. Mesoscale eddies in the South Atlantic Bight and the Gulf Stream Recirculation region: Vertical structure. *J. Geophys. Res. Oceans.* 2014, mars; 119(3):2048-2065.
DOI: 10.1002/2014JC009796.
 24. Liu Q et al. Observation-based source terms in the third-generation wave model wavewatch iii: updates and verification. *J. Phys. Oceanogr.* 2019, févr;49(2):489-517.
DOI: 10.1175/JPO-D-18-0137.1.
 25. Polnikov VG. The role of wind waves in dynamics of the air-sea interface. *Izv. Atmospheric Ocean. Phys.* 2009, juin; 45(3):346-356.

- DOI: 10.1134/S0001433809030086. of the stationary wind wave field. J. Phys. Oceanogr. 2019, janv;43(1):65-79.
26. Zavadsky A, Liberzon D, et L Shemer. Statistical analysis of the spatial evolution DOI: 10.1175/JPO-D-12-0103.1.

Disclaimer/Publisher's Note: The statements, opinions and data contained in all publications are solely those of the individual author(s) and contributor(s) and not of the publisher and/or the editor(s). This publisher and/or the editor(s) disclaim responsibility for any injury to people or property resulting from any ideas, methods, instructions or products referred to in the content.

© Copyright (2024): Author(s). The licensee is the journal publisher. This is an Open Access article distributed under the terms of the Creative Commons Attribution License (<http://creativecommons.org/licenses/by/4.0>), which permits unrestricted use, distribution, and reproduction in any medium, provided the original work is properly cited.

Peer-review history:
The peer review history for this paper can be accessed here:
<https://www.sdiarticle5.com/review-history/120245>